Doping dependence of charge-transfer excitations in $La_{2-x}Sr_xCuO_4$

Young-June Kim and J. P. Hill

Department of Physics, Brookhaven National Laboratory, Upton, New York 11973

Seiki Komiya and Yoichi Ando

Central Research Institute of Electric Power Industry,
2-11-1 Iwado-kita, Komae, Tokyo 201-8511, Japan

D. Casa, T. Gog, and C. T. Venkataraman

CMC-CAT, Advanced Photon Source, Argonne National Laboratory, Argonne, Illinois 60439
(Dated: February 2, 2008)

We report a resonant inelastic x-ray scattering (RIXS) study of the doping dependence of charge-transfer excitations in $La_{2-x}Sr_xCuO_4$. The momentum dependence of these charge excitations are studied over the whole Brillouin zone in underdoped (x=0.05) and optimally doped (x=0.17) samples, and compared with that of the undoped (x=0) sample. We observe a large change in the RIXS spectra between the x=0 and x=0.17 sample, while the RIXS spectra of the x=0.05 sample are similar to that of the x=0 sample. The most prominent effect of doped-holes on the charge excitation spectra is the appearance of a continuum of intensity, which exhibits a strong momentum-dependence below 2 eV. For the x=0.17 sample, some of the spectral weight from the lowest-lying charge-transfer excitation of the undoped compound is transferred to the continuum intensity below the gap, in agreement with earlier optical studies. However, the higher energy charge-transfer excitation carries significant spectral weight even for the x=0.17 sample. The doping dependence of the dispersion of this charge-transfer excitation is also discussed and compared with recent theoretical calculations.

PACS numbers: 74.25.Jb, 74.72.Dn, 78.70.Ck

I. INTRODUCTION

One of the central questions in the study of correlated electron systems is how the various types of electronic excitations evolve, as charge carriers are doped into Mott insulators. Most notably, the essential physics of the cuprate superconductors is generally regarded as that of a doped Mott insulator in two dimensions. For the spin degrees of freedom, magnetic neutron scattering has allowed the exploration of a large part of the phase space, and a detailed description of the doping dependence of the spin excitations now exists for many cuprate compounds. In particular, the incommensurate magnetic excitations in La-based cuprates are well known.[1,2,3] On the other hand, the situation for charge degrees of freedom is different. Although angle-resolved photoemission spectroscopy (ARPES) has provided a large amount of momentum-dependent information on the dispersion of a single quasiparticle,[4] collective charge excitations at nonzero momentum transfer are much less understood. This is due in large part to the lack of a suitable experimental probe, except for electron energy loss spectroscopy (EELS), which suffers from multiple scattering effects at large momentum transfers. On the other hand, at the zone center, there exist extensive optical spectroscopy studies of the doping dependence of the electronic excitation spectrum. For example, as holes are doped into La_2CuO_4, Uchida and coworkers[5] observed that the spectral weight is transferred from the charge-transfer (CT) excitation to low-energy excitations. The latter is composed of a Drude peak and a broad contin-

uum in the mid-infrared (MIR) range, which has yet to be understood.[6]

For a better understanding of the MIR band and other collective electronic excitations, it is necessary to also obtain information on the momentum dependence of these excitations. The resonant inelastic x-ray scattering (RIXS) technique in the hard x-ray regime has drawn interest in recent years, because it can provide just such momentum-dependent information about charge excitations.[7,8,9,10,11] In addition, since the penetration depth of hard x-rays is several microns, RIXS is a bulk probe, and can also accomodate magnetic fields and high pressures. Although RIXS probes valence electronic excitations, it has the additional benefit of element specificity, which is often associated only with core-level spectroscopies. Recently, we have reported the observation of two-dimensional (2D) CT excitations in insulating La_2CuO_4,[11] which is the parent compound of hole-doped $La_{2-x}Sr_xCuO_4$ (LSCO). In La_2CuO_4, the lowest energy excitation has a gap energy of 2.2 eV at the zone center, and exhibits a large (1 eV) dispersion. A second feature shows a smaller dispersion (0.5 eV) with a zone-center energy of 3.9 eV. It was argued that these are both highly-dispersive exciton-like modes, strongly damped by the presence of the electron-hole continuum. An alternative description of the observed spectra has recently been proposed by Nomura and Igarashi.[12] They attributed the observed two-peak feature to the fine structure of the Cu $3d$ partial density of states mixed with the O $2p$ band.

In order to address the question of how these dispersive charge excitations evolve as the system becomes metallic

via hole doping, we have carried out RIXS experiments on a lightly doped (x=0.05) sample and an optimally doped sample (x=0.17). As expected from the doping evolution of optical spectra[5], we observe the transfer of spectral weight from the lowest-lying CT exciton mode to a continuum at low energies. We also observe that there remains a significant spectral weight in the CT-like features around 4 eV, even in the x=0.17 sample. However, the onset energy of the CT excitation shifts to higher energy, and the low-energy CT exciton mode observed in the undoped sample seems to disappear in the optimally doped sample.

This paper is organized as follows. In the next section, we describe the experimental configurations used in the measurements, as well as the incident energy dependence of the RIXS spectra. Temperature and momentum dependence are discussed in Sec. III A and B, respectively. Our main results, the doping dependence of the low-energy charge excitations, are presented in Sec. III C. Finally, we discuss unresolved issues and possible future experiments in Sec. IV.

II. EXPERIMENTAL DETAILS

The experiments were carried out at the Advanced Photon Source on the undulator beamline 9ID-B. A double-bounce Si(111) monochromator and a Si(333) channel-cut secondary monochromator were utilized. A spherical (1 m radius), diced Ge(733) analyzer was used to obtain an overall energy resolution of 0.4 eV (FWHM).

Our choice of the LSCO system was based on its simple monolayer structure, and the fact that one can obtain large single crystals over a wide range of doping levels, which has enabled detailed characterization of all parts of the temperature-concentration phase diagram.[13] Although poor surface quality has limited ARPES study of these samples, a recent series of experiments by Ino and coworkers have provided a considerable amount of information about the valence band electronic structure.[14,15,16,17,18] Floating-zone grown single crystals of $La_{2-x}Sr_xCuO_4$ with x=0.17 and x=0.05 were used in our measurements. The as-grown samples were carefully anealed to remove excess oxygen. Their transport properties were reported previously.[19] The x=0.17 sample has $T_c \approx 42$ K, while the x=0.05 sample remains insulating down to low temperatures. The (100) plane of the x=0.17 crystal and the (110) plane of the x=0.05 crystal was cut and polished for the x-ray measurements. Throughout this paper, we use the tetragonal notation, with the **a/b** direction coinciding with the Cu-O-Cu bond direction. The scattering plane was vertical and the polarization of the incident x-ray was kept along the **c**-direction, that is perpendicular to the copper-oxygen plane. The x=0.17 sample was mounted on a closed-cycle refrigerator for the low-temperature measurements, while the x=0.05 sample was mounted on a room-temperature aluminium sample holder, which was evacuated to reduce the background
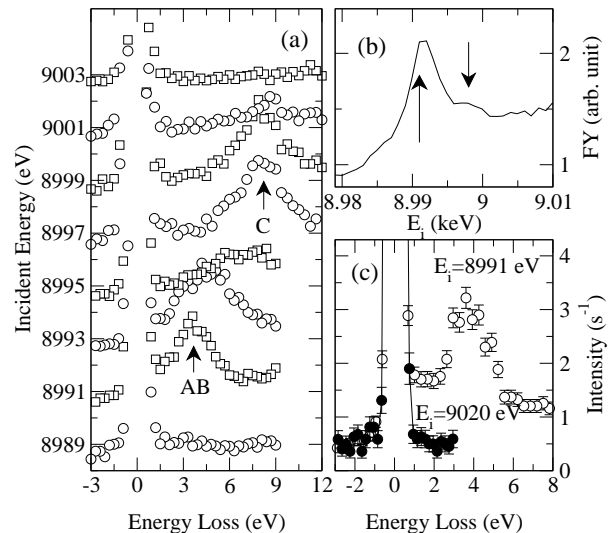

FIG. 1: (a) The RIXS intensity of the x=0.17 sample is plotted as a function of energy loss to show incident-energy dependence. The incident energy (E_i) of each scan is denoted on the left. (b) X-ray absorption spectrum monitored by fluorescence yield. Arrows denote the peak positions, where resonant enhancement are observed in the inelastic scattering. (c) Comparison of scattered intensity at two different incident energies. At resonance, $E_i = 8991$ eV, and far from resonance, $E_i = 9020$ eV. Data were taken at **Q**=(1 0 0).

from air scattering.

In Fig. 1(a), we plot the incident energy (E_i) dependence of the RIXS intensity for the x=0.17 sample as a function of energy loss ($\omega = E_i - E_f$) at a fixed momentum transfer of **Q**=(1 0 0). These data were taken at room temperature. The incident energy of each scan is denoted on the vertical axis. Since the **Q**=(1 0 0) position is a forbidden Bragg peak position, the elastic scattering intensty (i.e., at $\omega = 0$) is relatively small, enabling us to study the low-energy excitations in detail, even at the zone center. Two resonant features are observed in Fig. 1(a). As the incident energy is varied through $E_i \approx 8991$ eV, the low-energy feature around 3 eV shows a large resonant enhancement in the intensity. In order to compare the current data with those of the undoped sample,[11] this excitation is labeled AB. The second feature, labeled C, occurs around 8 eV and shows a markedly different resonance behavior, peaking at $E_i \approx 8997$ eV. Note that these two resonance energies correspond to peaks in the x-ray absorption spectra, (arrows in Fig. 1(b)). This latter was obtained by monitoring the fluorescence yield in the same experimental setup. We find that this resonance behavior for the x=0.17 sample is almost identical to that of undoped La_2CuO_4 as reported in Ref. 11. Similar resonance behavior was also observed for x=0.05 (not shown).

In Fig. 1(c), the $E_i = 8991$ eV scan is compared with that obtained with an incident photon energy of $E_i = 9020$ eV, i.e., much higher than the resonance energy.
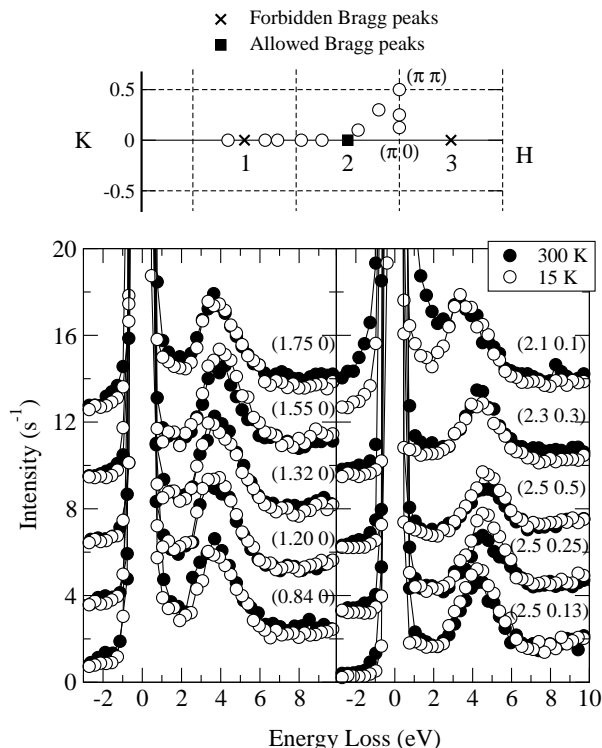
FIG. 2: RIXS intensity of LSCO (x=0.17) plotted as a function of energy loss at various momentum transfers. Scans are shifted vertically for clarity. Empty and filled symbols are data taken at $T = 15$ K and at $T = 300$ K, respectively. Schematic reciprocal space diagram is shown on top. The **Q**-positions where data were collected are denoted as circles.

This latter scan has little, or no resonant enhancement and represents, in some sense, the background scattering. From this comparison, one sees that there is significant resonant inelastic scattering down to 1 eV and lower. This resonant inelastic scattering is the subject of this paper. In the rest of this paper, the incident energy is held fixed either at 8991 eV or at 8997 eV, depending on the specific excitation being probed. We can then study the temperature, momentum, and doping dependence of these charge excitations in LSCO.

III. EXPERIMENTAL RESULTS

A. Temperature Dependence

In Fig. 2, representative RIXS scans, taken at various **Q** positions for the x=0.17 sample, are plotted as a function of ω. Here we have fixed the incident energy to 8991 eV, so that we can probe excitation AB. The out-of-plane component of the momentum transfer is held constant at $L = 0$, and **Q** is denoted for each scan as (HK). To note momentum transfer within a single Brillouin zone, we use the reduced wavevector, $\mathbf{q} \equiv \mathbf{Q} - \mathbf{G}$, where **G** is a

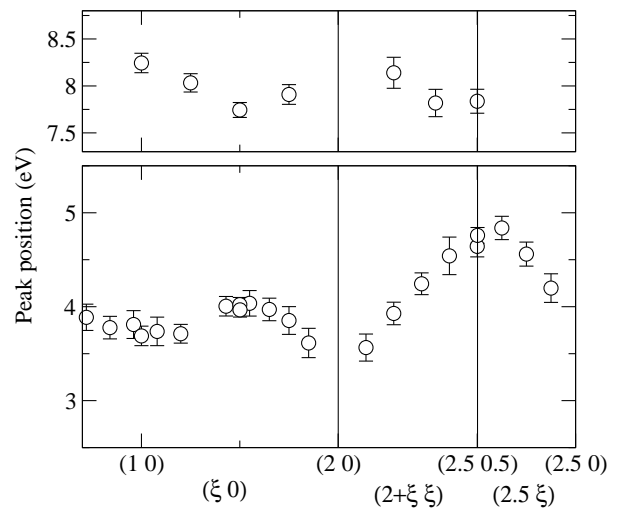

FIG. 3: Dispersion of the excitations measured at $T = 15$ K for LSCO (x-0.17). The top and bottom panels correspond to the low-energy (AB) and high-energy (C) excitations shown in Fig. 2 and Fig. 4, respectively.

reciprocal lattice vector. In the left panel, **q** is along the $(\pi\ 0)$ direction, with $(1\ 0)$ and $(2\ 0)$ being zone center positions. In the right panel, **q** along the $(\pi\ \pi)$ direction as well as along the zone boundary are shown. These positions are denoted as open symbols in the reciprocal space diagram shown on top of Fig. 2, in which the Brillouin zone boundaries are drawn as dashed lines.

Let us first consider the temperature dependence. We use filled and empty symbols in Fig. 2 to denote data taken at $T = 300$ K and $T = 15$ K, respectively. Clearly, there is little change in the RIXS spectra between the two temperatures, which is perhaps not surprising, given that the energy scale probed in these measurements is very large compared to thermal energies.[20] As the system is cooled down from room temperature, the only notable change is the reduced quasi-elastic tail, which has a large contribution from phonons. This effect is most clearly seen at the $(2.1\ 0.1)$ position, which is close to the $(2\ 0)$ Bragg peak position. This lack of observable temperature dependence in the charge excitation spectra justifies our later discussion, in which we compare data taken at different temperatures directly.

B. Momentum Dependence

The scans shown in Fig. 2 exhibit quite a large dispersion along the $(\pi\ \pi)$ direction, while the dispersion along the $(\pi\ 0)$ direction is smaller. We have fitted each scan to a Lorentzian peak with a sloping background, to obtain the peak position as a function of momentum transfer. This is plotted in the lower panel of Fig. 3, where the same notation for **Q** as that in Fig. 2 has been used. This excitation has a direct gap of ~ 3.7

4
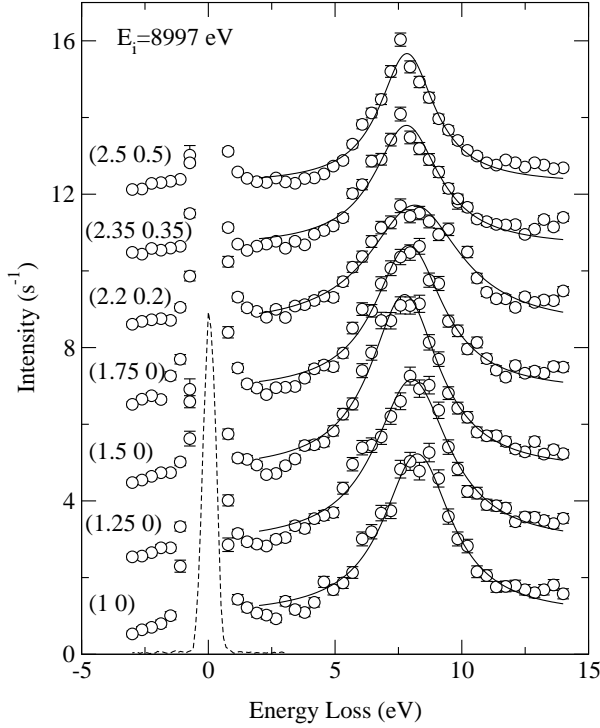

FIG. 4: RIXS intensity of LSCO obtained at various **Q** with the incident energy fixed at $E_i = 8997$ eV. Data are offset vertically for clarity. The dashed line is the intensity of the elastic scattering scaled to show the experimental energy resolution.

FIG. 5: Comparison of RIXS spectra at selected momenta for the x=0, x=0.05, and x=0.17 samples of $La_{2-x}Sr_xCuO_4$. The (0 0) and (π 0) data are shifted for clarity. The up and down arrows denote the onset energy of the spectra for the x=0.17 and x=0 samples, respectively.

eV; that is, the minimum energy position is the zone center, and the excitation disperses towards higher energy at the zone boundary: ~ 4 eV at (π 0), and ~ 4.7 eV at (π π). One should note that the dispersion displays significant anisotropy, which is also evident in the zone boundary dispersion from (2.5 0.5) to (2.5 0). Such a highly-dispersive excitation, AB, is reminiscent of the results obtained for La_2CuO_4, and, in both samples, originates from a particle-hole pair excitation across the CT gap. However, there are some differences between the spectra of the two samples, which will be discussed in the next section.

While excitation AB is resonantly enhanced for incident photon energies around $E_i = 8991$ eV, excitation C resonates around $E_i = 8997$ eV, as discussed above. It is believed to arise from the energy splitting between the bonding and antibonding molecular orbitals (MO) of the Cu-O bond. The observed spectra taken at this incident photon energy at various momentum transfers are shown in Fig. 4, with the same notation for **Q** as in Fig. 2. Excitation C is intrinsically very broad, when compared to the energy resolution (shown as the dashed line). We have therefore fitted each scan to a single Lorentzian peak, and obtained the peak position as a function of **Q**. This is plotted in the upper panel of Fig. 3. One can readily identify the finite bandwidth of excitation C:
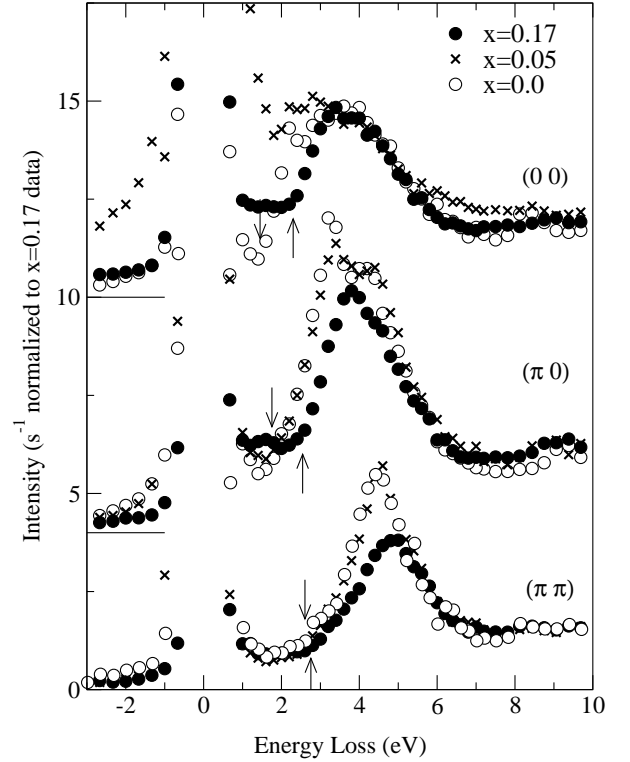
the difference between the excitation energy measured at (1 0) and (1.5 0) is about ~ 0.5 eV. It is interesting to note that this feature has a minimum energy at the zone boundary, either at (π,0) or (π,π). That is, excitation C has an indirect gap. Previously, we have reported that the excitation energy between the bonding MO and antibonding MO exhibits a systematic dependence on the Cu-O bond length.[21] Since a shorter bond-length results in stronger Cu $3d$ and O $2p$ hybridization, we expect the bonding-antibonding splitting to grow larger as the doping increases and the bond length decreases. Specifically, we observe a larger energy (~ 8 eV) for excitation C in LSCO (x=0.17) than in the x=0 sample, where an energy of ~ 7.3 eV was observed.[21] We attribute this to the shorter Cu-O bond length in the x=0.17 sample.

C. Doping Dependence

This section reports the main result of this paper. In Fig. 5, the RIXS spectra of the x=0, x=0.05, and x=0.17 samples are compared at three high-symmetry **q**-positions: (0 0), (π 0), and (π π). The data for the x=0 sample were previously reported in Ref. 11. The absolute **Q**-positions are (1 0 0), (2.5 0 0), and (2.5 0.5 0), from

top to bottom for the x=0 and x=0.17 samples. For the x=0.05 sample, the **Q**-positions correspond to (2 1 0), (2 1.5 0), and (1.5 1.5 0), respectively, since the surface of this sample was cut perpendicular to the [1 1 0] direction. In order to normalize the intensity between different samples, and between the spectra obtained at different momentum transfers, we monitored the fluorescence yield by measuring the Kβ_5 emission line at $E_f = 8973$ eV. The fluorescence yield was taken to be a measure of the volume of the sample being probed and any changes in this were used as normalization factors to scale the associated inelastic spectra. At **q**=(0 0) for the x=0 and x=0.17 samples, full emission spectra were measured and used for the normalization purpose, while for the other scans shown in Fig. 5, the intensity at the tail of Kβ_5 ($E_f \sim 8981$ eV) was used instead. Note that the (0 0) data for x=0.05 show a large low-energy background intensity from the elastic tail, since (2 1 0) is close to the allowed (2 1 1) Bragg reflection.

On a qualitative level, one can compare the **q**=(0 0) data in Fig. 5 with the optical conductivity data shown in Fig. 7 of Ref. 5. As La$_2$CuO$_4$ is doped with holes, the system becomes metallic and the insulating gap of the excitation spectrum is filled with spectral intensity, arising from the free-carrier contribution. However, there is a difference between the doping dependence of the optical conductivity and the RIXS spectra, especially at low-doping. In the optical conductivity data of Ref. 5, the gap is filled even at low doping of x=0.02 and x=0.06. For example, for x=0.02, the conductivity around ~ 1 eV grows quickly to about 60 % of the value for x=0.15. On the other hand, although limited in its scope, the RIXS data in Fig. 5 suggest very little change between the x=0 and x=0.05 sample, while the higher doping results are consistent with the optical data. However, one should be cautious in overinterpretating this data, since the relatively poor signal to noise ratio of the RIXS technique makes it less sensitive to small changes in spectral weight, when compared to optical conductivity. In addition, our sample geometry prevented us from obtaining good **q**=(0 0) data for the x=0.05 sample.

For x=0.17, we clearly observe a filling of the gap in the RIXS data, consistent with the behavior of the optical conductivity. Figure 1(c) shows that this gap-filling intensity is much larger than the background level. We note that the momentum dependence of the continuum intensity is quite strong. The gap-filling intensity in the region of $\omega < 2$ eV is significant at (0 0) and at (π 0), while this gap-filling intensity becomes very small at (π π). Possible origins of such momentum-dependent continuum excitations will be discussed in the next section.

For all doping levels, excitation AB is observed between $2 \sim 5$ eV. For a quantitative analysis of this scattering, we focus on the doping dependence of two quantities: the peak position and the onset energy of the spectral features. The first quantity can be straightforwardly determined by fitting the observed spectra to either one or two Lorentzian peaks. In Ref. 11, the x=0 data were
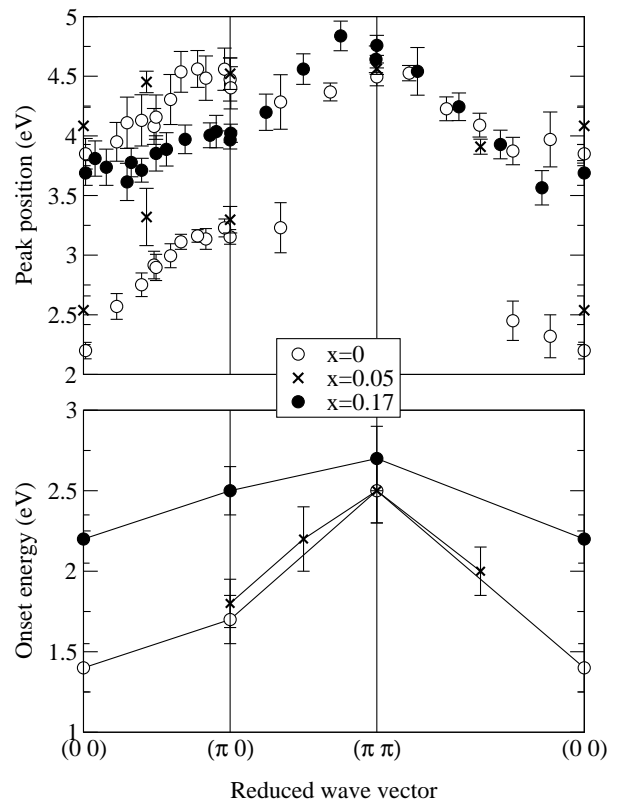

FIG. 6: Comparison of the dispersion relation of the low-energy charge excitation between the La$_{2-x}$Sr$_x$CuO$_4$ samples. The top panels show the dispersion of peak positions and the bottom panels show the dispersion of onset energies, as described in the text.

fitted with two peaks, the dispersion of which is reproduced as open circles in Fig. 6. Note that the spectral weight of the low energy peak becomes anomalously small around the (π π), leaving only a single peak around 4.5 eV. Our attempt to fit the x=0.17 data with two peaks was unsuccessful, and we have therefore fitted the spectra with a single Lorentzian with broad width, the peak position of which is plotted as filled circles in Fig. 6. We also have plotted a limited number of data points for the x=0.05 sample (crosses). As one can see in Fig. 6, the observed excitation of the x=0.17 data more or less falls in the energy range of the higher-energy excitation of the x=0 sample, which was labeled B in Ref. 11. A possible description, of this scattering, then, is that excitation A disappears while excitation B survives, as holes are doped into La$_2$CuO$_4$.

The onset energy of the spectral features, in contrast to the peak position, cannot be determined unambiguously, since this requires a precise knowledge of the background and the lineshape of the spectral feature. Therefore, we have attempted to determine this quantity consistently in the following way. For the x=0.17 sample, the gap-filling intensity at low energy is regarded as a constant, and the tail of the spectral feature is fitted to a linear line. The

crossing point of these two linear extrapolations is taken as the onset energy. For the x=0 and x=0.05 samples, the minimum intensity is used instead of the constant continuum intensity as a baseline, and a similar linear extrapolation was used to determine the onset energy. The onset energies determined in this way are noted in Fig. 5 (arrows), and are plotted in Fig. 6 as a function of momentum transfer for different doping levels. One can see that the onset energies also exhibit some dispersion, albeit smaller than that of the peak positions.

Upon hole-doping, the onset of excitation AB shifts to higher energy, with much smaller dispersion than that observed for the undoped sample. Excitation AB itself becomes broader and shows still sizable dispersion, especially along the $(0\ 0) - (\pi\ \pi)$ direction. However, the relatively sharp and well-defined exciton-like feature (A), observed around $2 \sim 3$ eV for x=0, is no longer visible in the x=0.17 sample. Since the doped charge-carriers screen the Coulomb interaction more effectively, it is reasonable to expect that the Coulomb interaction is no longer strong enough to create even the remnant of the exciton seen at x=0. Then the excitation AB observed for x=0.17 could be interpreted as a remainder of the higher energy (B) feature in the x=0 sample, though the width is broader than that of the undoped sample.

In our previous RIXS study of the undoped sample, we were not able to identify the nature of the higher energy feature, B. Two possibilities were suggested: One possibility is that it is also an exciton-like mode, but with a different symmetry. The second possibility is that feature B consists mainly of interband transitions from the valence band to conduction band. Given that the screening presumably prevents the low-energy exciton mode (A) from binding, our current observation of the CT feature seems to support the interband transition scenario. This interpretation is also consistent with the shift of onset energy with hole doping. Since the chemical potential now lies below the top of the valence band, a larger onset energy is required to excite a valence electron to the conduction band. This behavior of excitation AB is consistent with the cluster calculation carried out by Tsutsui *et al.*[22] In fact, if one takes the dispersion of the onset energy, intead of the center of gravity from Refs. 22 and 23, quantitative agreements are obtained between these calculations and the RIXS results. However, this agreement could be fortuitous, as discussed in the next section.

IV. DISCUSSION

There are three main differences observed in our RIXS study of LSCO (x=0.17 and x=0.05), when compared to the RIXS spectra of undoped La_2CuO_4. These are i) the appearance of the continuum intensity, ii) changes in the dispersion and energy scale of excitation AB, and iii) the shift of excitation C, which is identified as MO excitation. While the origin of iii) is believed to be mainly structural, the first two are results of charge carrier doping.

Among these, the low-energy continuum intensity, which fills the insulating gap, is straightforward to understand. Similar behavior has been observed with other spectroscopies, such as Raman scattering[24] and optical conductivity.[5] The gap-filling intensity is believed to arise from the incoherent creation of particle-hole pairs near the Fermi surface; that is, an intraband transition across the Fermi level. The momentum dependence of this gap-filling intensity, however, is difficult to understand. Specifically, the gap-filling intensity at $(\pi\ \pi)$ is very small compared to that at zone center, as shown in Fig. 5. In their study of the density-density correlation function of the t-J model, Tohyama and coworkers also observed similar anisotropic momentum-dependence of the low-energy spectral weight.[25]

One possible source of such anisotropy is the effect of the Fermi surface topology in intraband transitions. When transfering small momenta and energy, the transition probability of such an intraband transition can be quite large, since these transitions involve particle and holes in the same region of momentum space. However, in order to transfer large momenta, the particle and hole should come from different Brillouin zones. In this case, the shape of Fermi surface becomes important, and the transition probability can become very small. Such an effect could give rise to the momentum dependence of the very low energy spectral weight in LSCO. However, it is not clear if this effect can account for the observed momentum-dependence of the continuum intensity around $\omega \sim 1$ eV. More measurements with improved energy resolution are necessary to understand the momentum dependence of the continuum intensity.

Next, we note that the change in the AB feature is a result of two distinct phenomena. The first is the shift of chemical potential, which results in the shift of the AB feature to higher energy. The other is the disappearance of the lower energy CT exciton mode (mode A), presumably due to increased charge-carrier screening, and to the increased number of decay channels. Although our heuristic descriptions in the previous section provides reasonable accounts of these observations, a few questions still remain even on the qualitative level.

One issue is the momentum dependence of the onset energy, shown in Fig. 6. Despite the striking resemblance of this figure to the calculated results in Ref. 22, it was pointed out by Tsutsui *et al.* that LSCO should behave differently than the calculations, because the second and third nearest neighbor hoppings are much smaller in this material than those used in Ref. 22. In addition, the calculations showed that the bandwidth of the CT feature decreases in the hole-doped case, while in the electron-doped case it is almost the same as the undoped case. It was suggested that the rapid suppression of the antiferromagnetic correlations in hole-doped LSCO might be the reason for this smaller dispersion, since the antiferromagnetic correlation remains strong in electron-doped systems, such as $Nd_{2-x}Ce_xCuO_4$. However, one should note that, even at optimal doping, LSCO exhibits

strong antiferromagnetic fluctuations with a correlation length of $2 \sim 3$ lattice constants.[26] In fact, in underdoped LSCO systems, static magnetic order (stripes) has been observed at low temperatures, which implies that antiferromagnetic correlations in the hole-doped system are not negligible. Thus, if such correlations do play a role in the dispersion of the charge excitations, as suggested in Ref. 22, then the dispersion in LSCO would be expected to be closer to the undoped case.

To summarize, we have carried out a resonant inelastic x-ray scattering (RIXS) investigation of the doping dependence of charge excitations in LSCO. We observe a large change in the RIXS spectra between the x=0 and x=0.17 sample, while the RIXS spectra of the x=0.05 sample is similar to that of the x=0 sample. The most prominent effect of the doped-holes is the appearance of a continuum of intensity below 2 eV, which exhibits a strong momentum dependence. For x=0.17, some of the spectral weight from the charge-transfer excitation of the undoped compound is transferred to the continuum intensity below the gap, which is consistent with what has been observed in optical studies. However, the remainder

of the charge-transfer excitation carries significant spectral weight even for the x=0.17 sample. The observed doping-dependence of the dispersion of charge-transfer excitations seems to be broadly consistent with recent theoretical calculations.[22]

[1] R. J. Birgeneau and G. Shirane, in *Physical properties of high temperature superconductors I.*, edited by D. M. Ginsberg (World Scientific, Singapore, 1989), p. 151.
[2] S. W. Cheong, G. Aeppli, T. E. Mason, H. Mook, S. M. Hayden, P. C. Canfield, Z. Fisk, K. N. Clausen, and J. L. Martinez, Phys. Rev. Lett. **67**, 1791 (1991).
[3] K. Yamada, C. H. Lee, K. Kurahashi, J. Wada, S. Wakimoto, S. Ueki, H. Kimura, Y. Endoh, S. Hosoya, G. Shirane, R. J. Birgeneau, M. Greven, M. A. Kastner, and Y. J. Kim, Phys. Rev. B **57**, 6165 (1998).
[4] A. Damascelli, Z. Hussain, and Z. X. Shen, Rev. Mod. Phys. **75**, 1111 (2003).
[5] S. Uchida, T. Ido, H. Takagi, T. Arima, Y. Tokura, and S. Tajima, Phys. Rev. B **43**, 7942 (1991).
[6] E. Dagotto, Rev. Mod. Phys. **66**, 763 (1994).
[7] C. C. Kao, W. A. L. Caliebe, J. B. Hastings, and J. M. Gillet, Phys. Rev. B **54**, 16361 (1996).
[8] J. P. Hill, C. C. Kao, W. A. L. Caliebe, M. Matsubara, A. Kotani, J. L. Peng, and R. L. Greene, Phys. Rev. Lett. **80**, 4967 (1998).
[9] P. Abbamonte, C. A. Burns, E. D. Isaacs, P. M. Platzman, L. L. Miller, S. W. Cheong, and M. V. Klein, Phys. Rev. Lett. **83**, 860 (1999).
[10] M. Z. Hasan, E. D. Isaacs, Z. X. Shen, L. L. Miller, K. Tsutsui, T. Tohyama, and S. Maekawa, Science **288**, 1811 (2000).
[11] Y. J. Kim, J. P. Hill, C. A. Burns, S. Wakimoto, R. J. Birgeneau, D. Casa, T. Gog, and C. T. Venkataraman, Phys. Rev. Lett. **89**, 177003 (2002).
[12] T. Nomura and J. Igarashi, cond-mat/0312624.
[13] M. A. Kastner, R. J. Birgeneau, G. Shirane, and Y. Endoh, Rev. Mod. Phys. **70**, 897 (1998).
[14] A. Ino, T. Mizokawa, A. Fujimori, K. Tamasaku, H. Eisaki, S. Uchida, T. Kimura, T. Sasagawa, and K. Kishio, Phys. Rev. Lett. **79**, 2101 (1997).
[15] A. Ino, T. Mizokawa, K. Kobayashi, A. Fujimori, T. Sasagawa, T. Kimura, K. K. K. Tamasaku, H. Eisaki, and S. Uchida, Phys. Rev. Lett. **81**, 2124 (1998).
[16] A. Ino, C. Kim, T. Mizokawa, Z. X. Shen, A. Fujimori, M. Takaba, K. Tamasaku, H. Eisaki, and S. Uchida, J. Phys. Soc. Japan **68**, 1496 (1999).
[17] A. Ino, C. Kim, M. Nakamura, T. Yoshida, T. Mizokawa, Z. X. Shen, A. Fujimori, T. Kakeshita, H. Eisaki, and S. Uchida, Phys. Rev. B **62**, 4137 (2000).
[18] A. Ino, C. Kim, M. Nakamura, T. Yoshida, T. Mizokawa, A. Fujimori, Z. X. Shen, T. Kakeshita, H. Eisaki, and S. Uchida, Phys. Rev. B **65**, 094504 (2002).
[19] Y. Ando, A. N. Lavrov, S. Komiya, K. Segawa, and X. F. Sun, Phys. Rev. Lett. **87**, 017001 (2001).
[20] A significant temperature dependence of the RIXS spectra in manganites has recently been observed. S. Grenier *et al.* (unpublished)
[21] Y.-J. Kim, J. P. Hill, G. Gu, F. C. Chou, S. Wakimoto, R. J. Birgeneau, S. Komiya, Y. Ando, N. Motoyama, K. M. Kojima, S. Uchida, D. Casa, T. Gog, and C. T. Venkataraman, unpublished .
[22] K. Tsutsui, T. Tohyama, and S. Maekawa, Phys. Rev. Lett. **91**, 117001 (2003).
[23] K. Tsutsui, T. Tohyama, and S. Maekawa, Phys. Rev. Lett. **83**, 3705 (1999).
[24] S. Sugai, T. Ido, H. Takagi, S. Uchida, M. Sato, and S. Shamoto, Solid State Commun. **76**, 365 (1990).
[25] T. Tohyama, P. Horsch, and S. Maekawa, Phys. Rev. Lett. **74**, 980 (1995).
[26] R. J. Birgeneau, D. R. Gabbe, H. P. Jenssen, M. A. Kastner, P. J. Picone, T. R. Thurston, G. Shirane, Y. Endoh, M. Sato, K. Yamada, Y. Hidaka, M. Oda, Y. Enomoto, M. Suzuki, and T. Murakami, Phys. Rev. B **38**, 6614 (1988).